Electrical Power and Energy Systems 119 (2020) 105924

Contents lists available at ScienceDirect

Electrical Power and Energy Systems

journal homepage: www.elsevier.com/locate/ijepes

An alternative method for mitigating impacts of communication delay on load frequency control☆

Chang Fu[a], Caisheng Wang[a,*], Le Yi Wang[a], Di Shi[b]

[a] Electrical and Computer Engineering Department, Wayne State University, Detroit, MI 48202, USA
[b] 250 W. Tasman Dr.Ste 100, San Jose, CA 95134, USA

ARTICLE INFO

Keywords:
Communication delay
Delay margin
Load frequency control
Small gain theorem
Phase lead compensator

ABSTRACT

Load frequency control (LFC) has been considered as one of the most important frequency regulation mechanisms in modern power system. One of the inevitable problems involved in LFC over a wide area is communication delay. Not only can the delay deteriorate the system performance but also cause system instability. In this paper, an alternative design method is proposed to devise delay compensators for LFC in one or multiple control areas. For one-area LFC, a sufficient and necessary condition is given for designing a delay compensator. For multi-area LFC with area control errors (ACEs), it is demonstrated that each control area can have its delay controller designed as that in a one-area system if the index of coupling among the areas is below the threshold value determined by the small gain theorem. Effectiveness of the proposed method is verified by simulation studies on LFCs with communication delays in one and multiple interconnected areas with and without time-varying delays, respectively.

1. Introduction

Load frequency control (LFC) has been widely used in maintaining the balance between the load and generation in a specified control area and a large interconnected power system with multiple control areas over a wide region [1,2]. Dedicated communication channels have been used to transmit control signals between remote terminal units (RTUs) and a control center in a typical centralized LFC design. In such a traditional control scheme, most previous research work has ignored the problems due to communication delays [3]. Moreover, with the development of electricity market, the control processes involved in ancillary services require an open communication infrastructure that can rapidly respond to customers and utilities with large amounts of information exchanges [4]. How to efficiently integrate all the information, such as control, computing and communication, under deregulation and market environment has drawn lots of attention. It is urgent to have an open framework that fully considers communication delays to support such rising control needs. For instance, as introduced in [4], a new communication framework called GridStat has been introduced for data sharing. In this system, the impact of communication delays should be considered and carefully analyzed in order to maintain a secure and effective power system and market.

Time delay always exists in a communication network, Fig. 1, affecting the veracity and accuracy of information exchange and may degrade any control procedures chosen to stabilize the power grid [5]. In order to mitigate such negative impacts, various research efforts have been carried out recently [6–20]. A networked predictive control approach considering the round-trip time delay in the feedback loop was studied in [6] for wide-area damping control in power system inter-area oscillations. In [7], the LFC problem was formulated as a constrained optimization problem and a robust PI controller was designed for time delay compensation. Genetic Algorithm (GA) was used in [8] for controller design in a single area LFC with time delays. However, these approaches require the entire system information. Thus, the computational cost will increase significantly when the system size increases. The computation efficiency of delay involved LFC control design was studied in [9]. By decreasing both the number of decision variables and the maximal order of the LMI, the calculation burden was significantly reduced. However, there are concerns on the reconstructed model that it might not be able to represent the characteristics of the original system. An event-trigger control method was introduced in [10] to update the PI controller parameters regarding different communication delays; however, the responses of PI control can vary due to the characteristic of the system. In [11], a model predictive controller and a Smith predictor-based controller were proposed to overcome delays in communication channels in frequency restoration in an islanded

☆ This work was supported in part by the National Science Foundation of USA under Grant ECCS-1508910.
* Corresponding author.
E-mail addresses: chang.fu@wayne.edu (C. Fu), cwang@wayne.edu (C. Wang), lywang@wayne.edu (L.Y. Wang), di.shi@geirina.net (D. Shi).

https://doi.org/10.1016/j.ijepes.2020.105924
Received 18 November 2019; Received in revised form 31 January 2020; Accepted 4 February 2020
0142-0615/

Nomenclature

β	Frequency bias factor.
$\Delta\omega$	Frequency deviation (p.u.).
ΔP_L	Load change, independent of ω (p.u.).
ΔP_m	Mechanical power output change (p.u.).
ΔP_v	Valve position change (p.u.).
δ_{ij}	Phase angle difference between buses i and j at the equilibrium point.
ω_0	Synchronous radian frequency (p.u.).
ω_c	Gain-crossover frequency (rad/s).
τ	Communication delay (s).
τ_m	Communication delay margin (s).
τ_{max}	Maximum communication delay (s).
τ_{min}	Minimum communication delay (s).
ACE	Area control error (p.u.).
D	Ratio of the percent change in load over ω (%).
$D_{i,o}$	Value of D with the original base in Area i.
$D_{ik,o}$	Value of D with the kth generator in Area i.
G_c	Phase-lead compensator.
H	Inertia constant (s).
H_{ii}	Transfer function from input of area i to the output of area i.
H_{ij}	Transfer function from input of area i to the output of area j.
I_n	Coupling index for an n-area LFC schem.
K_{Ii}	The integral controller in the ith area.
LMI	Linear Matrix Inequality.
M	$M = 2H$ (s).
n_i	Number of generators in Area i.
P_{tie_i}	The tie-line power from the ith area.
R	Governor speed regulation droop coefficient (p.u.).
T_g	Governor constant (s).
T_{ch}	Turbine time constant (s).
T_{ij}	Synchronizing power coefficient of tie-line ij (p.u./rad).
V_i, V_j	Per unit voltage at bus i and j.

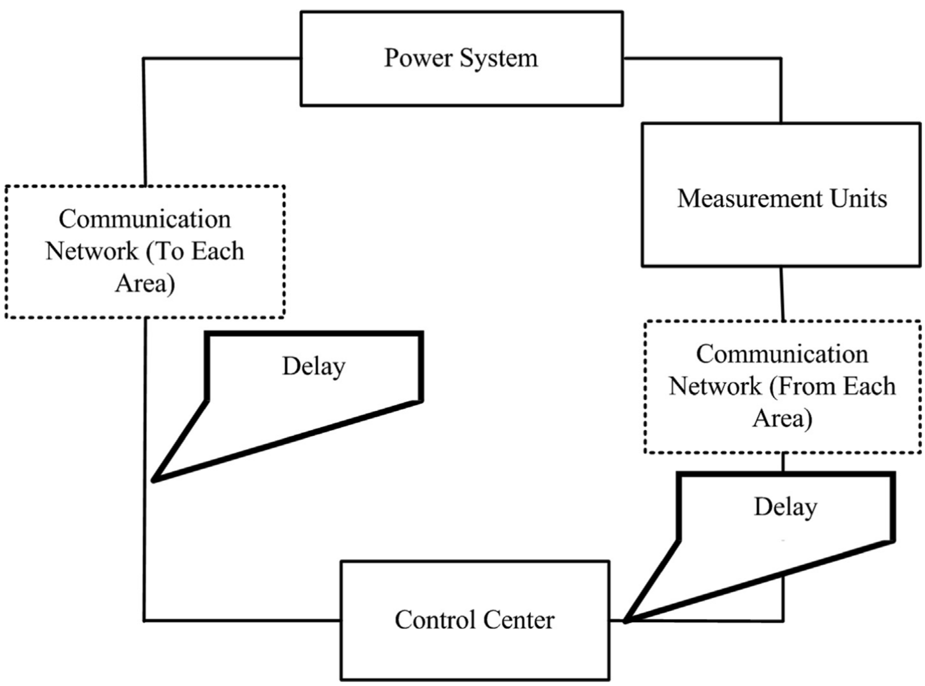

Fig. 1. Communication delay in LFC control.

microgrid. These delays usually range from milliseconds to tens of milliseconds, which are small compared to those that can happen in a large area LFC system. LMI approaches were widely used in recent years for handling delay issues in LFC control. In [12,13], LMI based control approaches were proposed and claimed to be robust with respect to communication delays and failures. A novel Lyapunov-Krasovski function was used in [13] for providing less conservative than Wirtinger's inequality. Another LMI approach was taken in [14] to investigate the delay-dependent stability of an LFC scheme with constant and time-varying delays. The delay margins for PI-type controllers in one-area and multi-area LFC schemes were obtained in [15], where a robust, PID-type LFC control strategy was proposed to deal with time-varying delays. In [16], a delay margin estimation approach was provided for a robust LFC control. An approach for designing an optimum gain of a PID controller subject to LMI was presented in [17] to improve the dynamic response performance. In [18], an LMI based robust predictive LFC control was proposed by considering lower computational complexity. The LMI approach has also been used in H_∞ control to design a delay-dependent controller for stabilizing the system with multiple delays in different areas in [19]. Another LMI based H_∞ controller design was presented for power systems where the system states have uncertain delays with the delay upper boundary known as constant values [20].

However, an LMI based method only provides a sufficient condition of stability. If the LMI stability criterion is not met, it is still not clear whether the system is stable or not [21]. Therefore, it is important to find a way to design a controller in which the necessary and sufficient condition of stability can be met. Furthermore, the complexity of the design will be significantly increased if the number of areas in the system increases. Therefore, it is also worthy to find an approach that can simplify the design procedure for multi-area cases. The contribution of this paper can be found as follows:

1. The impact of delay on LFC is firstly analyzed in the frequency domain through a classic approach. Different from LMI approach, a sufficient and necessary condition is given for designing a delay

compensator for a one-area LFC scheme and then extended to multi-area LFC schemes that cover a wide region with constant and time-varying communication delays.

2. Impacts on frequency regulation and the corresponding delay compensator design due to the coupling among different areas connected via tie lines are fully investigated. It is demonstrated that the delay compensator for each control area can still be designed in a simpler approach, in which only local system information is needed to design such controller, if the index of coupling among the areas is below the threshold value determined by the small gain theorem [22].

The remainder of this paper is organized as follows: Models of one-area and multi-area LFC schemes with communication delays are reviewed in Section 2. The design of controller to compensate the communication delay impacts is given in Section 3. Simulation studies are carried out and discussed in Section 4 to verify the effectiveness of the proposed method. Comparison of the proposed approach and LMI metheds, as well as the impacts of coupling among different areas in a power system with multiple control areas are presented in Section 5, followed by the conclusions drawn in Section 6.

2. LFC schemes with communication delays

A large, interconnected power system can have several control areas. A control area, also called balancing authority area, consisting of a set of generation, transmission assets and loads within its territory, is responsible for maintaining load balancing of the area and supports the area's interconnection frequency in real time [1]. Dynamic models of one-area LFC and multi-area LFC schemes with communication delays are reviewed in this section. Communication delays usually arise when signals are transmitted between the control center and individual units, such as when telemetered signals are exchanged between RTUs and the control center for signal processing and control law updating, etc. [15]. For the purpose of analysis, in this paper, all delays are considered as an overall equivalent delay τ in both one-area and multi-area LFC schemes [3].

2.1. One-area LFC model

The dynamic model of a typical one-area LFC scheme is shown in Fig. 2. Detailed model of a typical LFC scheme can be found in [1]. Without considering the delay $e^{-\tau s}$ and the delay compensator G_c, the system state-space model can be written as [14]:

$$\begin{cases} \dot{x}(t) = Ax(t) + Bu(t) + F\Delta P_L(t) \\ y(t) = Cx(t) \end{cases} \tag{1}$$

where

$$x(t) = [\Delta\omega \quad \Delta P_v \quad \Delta P_m \quad \int ACE]^T$$
$$y(t) = [\Delta\omega]$$
$$A = \begin{bmatrix} -D/M & 0 & 1/M & 0 \\ -1/T_g R & -1/T_g & 0 & -K_I/T_g \\ 0 & 1/T_{ch} & -1/T_{ch} & 0 \\ \beta & 0 & 0 & 0 \end{bmatrix}$$
$$B = [0 \quad 1/T_g \quad 0 \quad 0]^T$$
$$F = [0 \quad -1/M \quad 0 \quad 0]^T$$
$$C = [1 \quad 0 \quad 0 \quad 0]$$

where $u(t)$ is the control signal sent from the control center. Due to no tie-line power exchanges in the one-area LFC scheme, the ACE signal is described as Eq. (2):

$$ACE = \beta\Delta\omega \tag{2}$$

where $\beta = 1/R + D$. The total equivalent communication delay is represented as $e^{-\tau s}$ in Fig. 2. By defining a new virtual state q, as shown in Fig. 2, the following equations can be obtained:

$$\begin{aligned} q(t) &= [1 \quad 1]\begin{bmatrix} g(t-\tau) \\ u(t-\tau) \end{bmatrix} \\ &= [1 \quad 1]\begin{bmatrix} C''x(t-\tau) \\ u(t-\tau) \end{bmatrix} \end{aligned} \tag{3}$$

$$C'' = [0 \quad 0 \quad 0 \quad -K_I]$$

In addition, the state-space representation of the controller G_c, which is to be designed in Section 4.1, can be written as:

$$\begin{cases} \dot{z}(t) = A_c z(t) + B_c q(t) \\ w(t) = C_c z(t) + D_c q(t) \end{cases} \tag{4}$$

where A_c, B_c, C_c, D_c vary according to different G_c controllers. Substituting (3) and (4) into (1), the delayed system including the compensator can be written as Eq. (5):

$$\begin{cases} \dot{f}(t) = A'f(t) + A_d f(t-\tau) + B'u(t-\tau) + F'\Delta P_L(t) \\ y(t) = C'x(t) \end{cases} \tag{5}$$

where

$$\begin{aligned} & f(t) = \begin{bmatrix} x(t) \\ z(t) \end{bmatrix} A' = \begin{bmatrix} A & BC_c \\ 0 & A_c \end{bmatrix} \\ & A_d = \begin{bmatrix} BD_c C'' & 0 \\ B_c C'' & 0 \end{bmatrix} \\ & B' = \begin{bmatrix} BD_c \\ B_c \end{bmatrix} \\ & F' = \begin{bmatrix} F \\ 0 \end{bmatrix} \\ & C' = [C'' \quad 0] \end{aligned} \tag{6}$$

The one-area LFC can be represented as a single-input-single-output (SISO) system and thus the transfer function can be readily obtained. The frequency domain analysis will be carried out later for the controller design to mitigate the impact of delay.

As shown in Fig. 2, the delay compensator is designed for the entire system that includes an integral controller (i.e., I controller) used in the

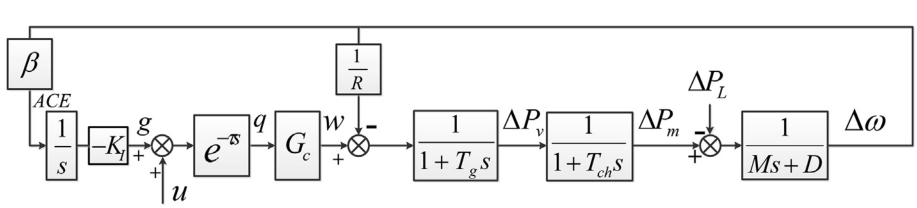

Fig. 2. One-area LFC scheme with communication delay.

LFC to help regulate frequency. Actually, for the delay compensator design, it does not matter if some other type of controller such as a PI or PID controller is used in the original system.

2.2. Multi-area LFC model

The dynamic model of a multi-area LFC scheme with n control areas is shown in Fig. 3. The system state space model without considering the delay can be obtained as Eqs. (7)–(9) [10]:

$$\begin{cases} \dot{x}(t) = Ax(t) + Bu(t) + F\Delta P_L(t) \\ y(t) = Cx(t) \end{cases} \tag{7}$$

where

$$x(t) = [x_1 \ \cdots \ x_i \ \cdots \ x_n]^T$$
$$y(t) = [y_1 \ \cdots \ y_i \ \cdots \ y_n]^T$$
$$u(t) = [u_1 \ \cdots \ u_i \ \cdots \ u_n]^T$$

$$x_i(t) = [\Delta\omega_i \ \ \Delta P_{vi} \ \ \Delta P_{mi} \ \ \textstyle\int ACE \ \ \Delta P_{tiei}]^T$$
$$y_i(t) = [\Delta\omega_i] \tag{8}$$

$$\Delta P_L(t) = [\Delta P_{L1}(t) \ \cdots \ \Delta P_{Li}(t) \ \cdots \ \Delta P_{Ln}(t)]^T$$

$$A = \begin{bmatrix} A_{11} & \cdots & A_{1i} & \cdots & A_{1n} \\ \vdots & \ddots & \vdots & \ddots & \vdots \\ A_{i1} & \cdots & A_{ii} & \cdots & A_{in} \\ \vdots & \ddots & \vdots & \ddots & \vdots \\ A_{n1} & \cdots & A_{ni} & \cdots & A_{nn} \end{bmatrix}$$
$$B = diagB_i, \ C = diagC_i$$

$$F = diagF_i, \ B_i = [0 \ \ 1/T_{gi} \ \ 0 \ \ 0 \ \ 0]^T \tag{9}$$

$$A_{ii} = \begin{bmatrix} -D_i/M_i & 0 & 1/M_i & 0 & -1/M_i \\ 1/T_{gi}R_i & 1/T_{gi} & 0 & -K_{Ii}/T_{gi} & 0 \\ 0 & 1/T_{chi} & -1/T_{chi} & 0 & 0 \\ \beta_i & 0 & 0 & 0 & 1 \\ E_i & 0 & 0 & 0 & 0 \end{bmatrix}$$

$$A_{ij} = \begin{bmatrix} 0 & 0 & 0 & 0 & 0 \\ 0 & 0 & 0 & 0 & 0 \\ 0 & 0 & 0 & 0 & 0 \\ 0 & 0 & 0 & 0 & 0 \\ -\omega_0 T_{ij} & 0 & 0 & 0 & 0 \end{bmatrix}$$
$$F_i = [0 \ \ 1/M_i \ \ 0 \ \ 0 \ \ 0]^T$$
$$C_i = [1 \ \ 0 \ \ 0 \ \ 0 \ \ 0]$$
$$,E_i = \omega_0 \sum_{j=1, j\neq i}^{n} T_{ij}$$

Notations are similar to those used in one-area LFC but with subscript i for Area i in a multi-area system. Subscript j is used for the signals from another area (i.e., the jth area) that is connected to area i via a tie line. All control areas are denoted by $1, 2, \ldots, n$. The ACE signal can be represented as:

$$ACE_i = \Delta P_{tiei} + \beta_i \Delta\omega_i$$

The delayed system with n sub-areas can be represented as Eq. (10):

$$\begin{cases} \dot{f}(t) = A'f(t) + \sum_{i=1}^{n} A_{di} f(t-\tau_i) + B'u(t-\tau_i) + F'\Delta P_L(t) \\ y(t) = C'x(t) \end{cases} \tag{10}$$

where

$$A_{di} = diag\left[0 \cdots \begin{bmatrix} B_i D_{ci} C''_i & 0 \\ B_{ci} C''_i & 0 \end{bmatrix} \cdots 0\right]$$
$$u(t) = [u_1 \ \cdots \ u_i \ \cdots \ u_n]^T, \quad C' = diag[C'_i]$$
$$C'_i = [C''_i \ \ 0], \quad C''_i = [0 \ \ 0 \ \ 0 \ \ -K_{Ii} \ \ 0]$$
$$B' = diag[B'_1 \ \cdots \ B'_i \ \cdots \ B'_n]$$

Other notations are the same as those in (6) with subscript i indicating area i.

3. Load frequency control design with communication delay

Systems shown in Figs. 2 and 3 are linear time invariant (LTI) systems when delays do not present. Hence, the impact of delay can be analyzed via a classic approach. For SISO system shown in Fig. 2, a necessary and sufficient condition can be obtained for designing a controller to guarantee the stability of the system. It is, however, challenging to analyze a large power system with coupled control areas, which is in general a multi–input-multi–output (MIMO) system as shown in Fig. 3. The interactions among different control areas in a multi-area LFC are discussed in this section. The small gain theorem [22] is used to demonstrate and verify that the delay compensator for each control area can be designed independently in the way as in a single one-area system if the coupling index among different areas is below the threshold value (more discussions given later in this section).

3.1. Delay margin

For a SISO LTI and open-loop stable system, its transfer function is assumed to be $G(s)$ and the frequency response is $G(j\omega)$ when there is no delay. If the gain crossover frequency of this delay-free system is ω_c, the corresponding phase margin will be $\varphi_\omega = \angle(j\omega_c) + 180°$ .When a delay of τ is introduced to the open-loop system, the delay does not change the gain curve, and hence the new gain crossover frequency of the system is still ω_c. Nevertheless, the delay introduces an extra phase lag of $-\tau\omega_c$, at ω_c, leading to a new phase margin, $\varphi_{new} = \varphi_\omega - \tau\omega_c$. The Nyquest stability criterion, which is necessary and sufficient in this case, implies that the maximum permitted time delay for stability is given by $\varphi_{new} = 0$, which implies $\varphi_\omega - \tau_m \cdot \omega_c = 0$, or $\tau_m = \varphi_\omega/\omega_c$ [23,24]. Therefore, it is a necessary and sufficient condition that the closed system with time delay is stable when the delay $\tau \leqslant \tau_m$.

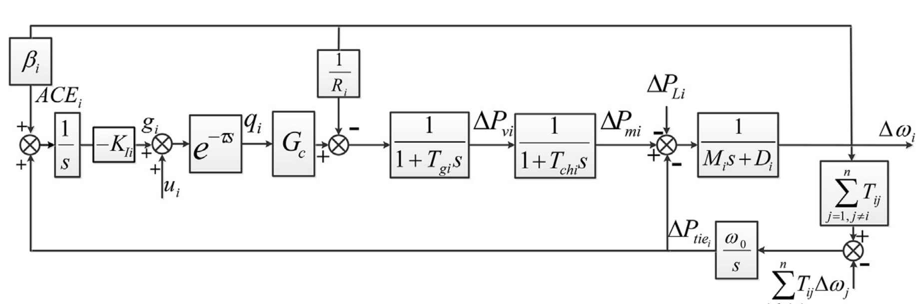

Fig. 3. Area i in a multi-area LFC scheme with communication delay.

3.2. Compensator design for one-area LFC with communication delay

The one-area LFC scheme shown in Fig. 2 is a SISO system. The communication delay exists in the system can be treated as one equivalent delay in the transmission of ACE [14]. Let $G(s)$ be the open-loop system transfer function without delay and the delay compensator. $G(s)$ can be derived from its state space model in (1). Let $e^{-\tau s}$ be the communication delay, and $G_c(s)$ be the compensator to be designed. The design of a phase lead compensator is given below as an illustrative example. For system $G(s)$, the structure of the phase lead compensator can be written as [24]:

$$G_c(s) = \alpha\frac{s + 1/\alpha T}{s + 1/T} \tag{11}$$

Denoting $\varphi_{\omega d}$ as the desired phase margin, $\varphi_{\omega u}$ as the uncompensated phase margin, and $\varphi_{\omega s}$ as the safety factor, α can be calculated based on Eq. (12) [24]:

$$\alpha = \frac{1 + sin\varphi}{1 - sin\varphi} \tag{12}$$

where $\varphi = \varphi_{\omega d} - \varphi_{\omega u} + \varphi_{\omega s}$. The compensator will lift the magnitude upwards by $10{\cdot}log_{10}(\alpha)$ dB at ω_m, where ω_m is the corner frequency of (11). Choose ω_m as the new gain-crossover frequency of the compensated system to maximize the phase margin compensation. That is $|G_c(j\omega_m)G(j\omega_m)| = 0$ dB. In other words, $|G(j\omega_m)|_{dB} = -10{\cdot}log_{10}(\alpha)$. Once the frequency ω_m is identified, the compensator $G_c(s)$ can be calculated based on $\frac{1}{T} = \sqrt{\alpha}\,\omega_m$.

3.3. Multi-area LFC with communication delays

In a multi-area LFC scheme, due to different load changes in different areas, and tie-line power interactions, the controller design becomes an MIMO system based design and the couplings among individual areas need to be studied carefully. On the one hand, since different control areas are linked together via tie-lines, load change in one area will also impact the other areas. Moreover, each area has its own ACE based control and one of the control objectives is to maintain the power flows at a given level along the tie-lines. In other words, under a certain equilibrium point, each control area is controlled to take care of its own load changes unless a new set of tie-line power references are issued. Therefore, if different areas are "not strongly coupled", the delay compensator design procedure for a MIMO system can still follow the one developed for the one-area LFC scheme. It is worthwhile to mention that a criterion (the condition of (18)) will be developed later in this section to check whether the areas in a multi-area system are strongly coupled or not. As discussed in Sections 4 and 5, many multi-area systems with highly integrated areas via tie lines meet the criterion of (18). That is, the delay compensator for each control area can still be designed independently if the condition of (18) is satisfied. This is a decentralized delay compensation scheme. We will use the small gain theorem [22] to analyze the couplings among different sub-systems in an MIMO system.

The equivalent diagram of a multi-area LFC scheme is shown in Fig. 4. For a single area in the figure, e.g., Area 1, the area topology can be represented by a feedback transfer function H_{11} and a forward transfer function G_1. H_{11} and G_1 are derived according to Fig. 3 without considering the impact from other areas. The impacts from the ith area to Area 1 are, however, represented by two parts: H_{i1} and C_{i1}. The C_{i1} is the transfer function indicating signal from $\Delta\omega_i$ to $\Delta\omega_1$, which can be derived by Mason's Rule. The feedback from area i to this area (Area 1), shown as H_{i1} in the lower part of Fig. 4, is presented as $H_{i1} = K_{Ii}T_{i1}\omega_0/s^2$. The overall impact from all other areas to Area 1 can thus be represented as $\sum_{j=2}^{n} H_{j1}\Delta\omega_j$ (the feedback to the input) and $\sum_{j=2}^{n} C_{i1}\Delta\omega_j$ (to the output), shown in Fig. 4.

Taking a two-area LFC scheme for instance, a more generic diagram representation is shown in Fig. 5. H_{12} and H_{21} are the feedback transfer functions from $\Delta\omega_1$ to Area 2 and $\Delta\omega_2$ to Area 1, respectively. The relationship between the inputs $\boldsymbol{u}$ and outputs $\boldsymbol{y}$ can be found in (13).

$$\begin{bmatrix} y_1 \\ y_2 \end{bmatrix} = \boldsymbol{P_2}\begin{bmatrix} u_1 \\ u_2 \end{bmatrix} - \boldsymbol{M_2}\begin{bmatrix} y_1 \\ y_2 \end{bmatrix} \tag{13}$$

where

$$\boldsymbol{M_2}=\begin{bmatrix} G_1G_{c1}e^{-\tau_1 s}H_{11} & G_1G_{c1}e^{-\tau_1 s}H_{21} - C_{21} \\ G_2G_{c2}e^{-\tau_2 s}H_{12} - C_{12} & G_2G_{c2}e^{-\tau_2 s}H_{22} \end{bmatrix}$$

$$\boldsymbol{P_2}=\begin{bmatrix} G_1G_{c1}e^{-\tau_1 s} & 0 \\ 0 & G_2G_{c2}e^{-\tau_2 s} \end{bmatrix}$$

The closed-loop transfer function of the two-area LFC scheme can be obtained as:

$$\boldsymbol{y} = (\boldsymbol{I} + \boldsymbol{M_2})^{-1}\boldsymbol{P_2}{\cdot}\boldsymbol{u} \tag{14}$$

The stability criteria of system in (14) is that $[\boldsymbol{I} + \boldsymbol{M_2}]^{-1}$ is stable, since $\boldsymbol{P_2}$ is stable.

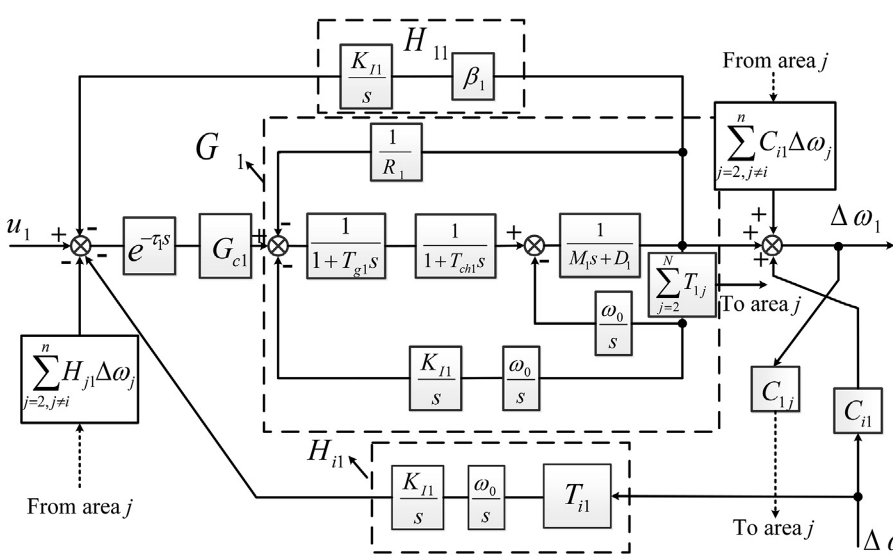

Fig. 4. Area 1 to the ith area of a multi-area LFC scheme.

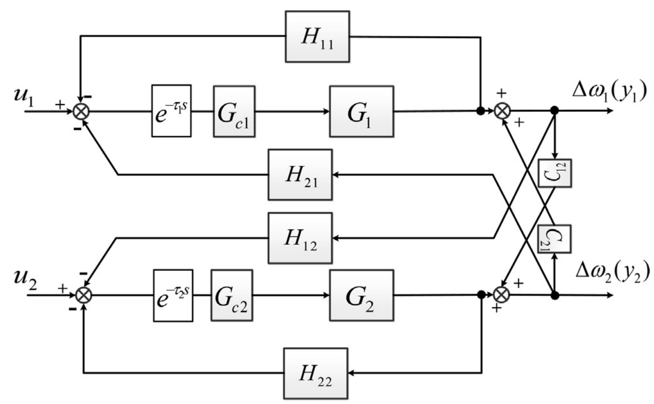

Fig. 5. A generic two-area LFC scheme.

$$(\boldsymbol{I}+\boldsymbol{M_2})^{-1}=\left(\begin{bmatrix}1+G_1G_{c1}e^{-\tau_1 s}H_{11} & 0\\ 0 & 1+G_2G_{c2}e^{-\tau_2 s}H_{22}\end{bmatrix}+\begin{bmatrix}0 & G_1G_{c1}e^{-\tau_1 s}H_{21}-C_{21}\\ G_2G_{c2}e^{-\tau_2 s}H_{12}-C_{12} & 0\end{bmatrix}\right)^{-1}$$

Let

$$\boldsymbol{N_2}=\begin{bmatrix}1+G_1G_{c1}e^{-\tau_1 s}H_{11} & 0\\ 0 & 1+G_2G_{c2}e^{-\tau_2 s}H_{22}\end{bmatrix}$$

$$\boldsymbol{\Delta_2}=\begin{bmatrix}0 & G_1G_{c1}e^{-\tau_1 s}H_{21}-C_{21}\\ G_2G_{c2}e^{-\tau_2 s}H_{12}-C_{12} & 0\end{bmatrix}$$

$(\boldsymbol{I}+\boldsymbol{M_2})^{-1}$ can thus be written as $[\boldsymbol{N_2}+\Delta_2]^{-1}$. This can be further written as $[\boldsymbol{I}+\boldsymbol{N_2^{-1}}\Delta_2]^{-1}\boldsymbol{N_2^{-1}}$. $\boldsymbol{N_2^{-1}}$ is stable due to the local stability: the diagonal elements in $\boldsymbol{N_2^{-1}}$ are the denominators of the closed loop transfer function of each subsystem, and all the subsystems are assumed to be stable. Define the coupling index I_2 of this two-area LFC scheme as $||\boldsymbol{N_2^{-1}}\Delta_2||_\infty$. In order to determine the stability of (14),

$$I_2=||\boldsymbol{N_2^{-1}}\Delta_2||_\infty<1 \tag{15}$$

should be satisfied [25].

Eq. (15) can be further written as Eq. (16):

$$||\boldsymbol{N_2^{-1}}\Delta_2||_\infty\leqslant||\boldsymbol{N_2^{-1}}||_\infty\cdot||\Delta_2||_\infty<1 \tag{16}$$

Thus, the stability criteria of system in (14) is Eq. (17):

$$||\Delta_2||_\infty<\frac{1}{||\boldsymbol{N_2^{-1}}||_\infty} \tag{17}$$

The discussion on the two-subsystem system can be extended to a multi-area system (e.g., an n-area LFC scheme). The coupling index I_n is defined as $||\boldsymbol{N_n^{-1}}\Delta_n||_\infty$, and the stability is determined by (18):

$$I_n=||\boldsymbol{N_n^{-1}}\Delta_n||_\infty<1 \tag{18}$$

or equivalently

$$||\boldsymbol{\Delta_n}||_\infty<\frac{1}{||\boldsymbol{N_n^{-1}}||_\infty} \tag{19}$$

where

$$\boldsymbol{N_n}=diag\,[1+G_iG_{ci}e^{-\tau_i s}H_{ii}]$$

$$\boldsymbol{\Delta_n}=\begin{bmatrix}0 & \cdots & G_nG_{cn}e^{-\tau_1 s}H_{n1}-C_{n1}\\ \vdots & \ddots & \vdots\\ G_iG_{ci}e^{-\tau_i s}H_{1i}-C_{1i} & \cdots & G_iG_{ci}e^{-\tau_i s}H_{ni}-C_{ni}\\ \vdots & \ddots & \vdots\\ G_nG_{cn}e^{-\tau_n s}H_{1n}-C_{1n} & \cdots & 0\end{bmatrix}$$

4. Simulation study

Simulation studies are carried out for both one-area and multi-area LFC schemes to verify the proposed method. A one-area LFC based phase lead compensator design considering a constant communication delay is first discussed to illustrate the proposed precedure. The design is then extended to the multi-area LFC scheme with multiple time-varying communication delays in different sub-areas.

Table 1
Parameters of one-area LFC scheme.

Parameters	M	D	β	R	K_I	T_g	T_{ch}	ΔP_L
Area$_1$	10	0.8	20.8	0.05	7	0.2	0.5	0.2

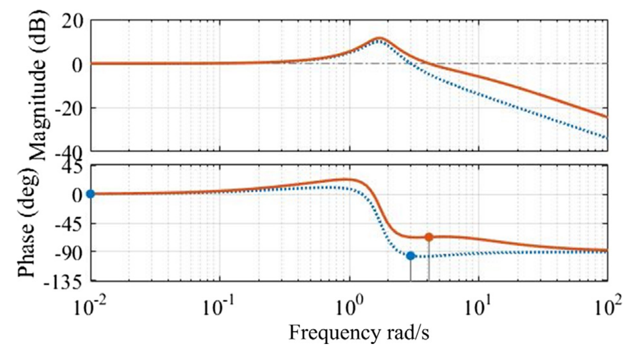

Fig. 6. Bode plot of the original system (Dash) and the compensated system (Solid).

4.1. One-area LFC

Parameters for the one-area LFC are shown in Table 1 [1]. Bode plots show that the phase margin ω_m and crossover frequency can be readily obtained according to Fig. 6 (dotted line). Using the design procedure described in Section 3.2, choose $K_c=1$ and $\varphi=30°$ for instance, it is easy to get $\alpha=3$ and $|G(j\omega_m)|_{dB}=-10\cdot log_{10}(\alpha)=-4.7$dB [26,27]. The frequency is found to be $\omega_c=4.1$ rad/s at that amplitude. Therefore, $1/T$ and $1/\alpha T$ in (11) can be calculated as 7.1 rad/s and 2.37 rad/s, respectively. Therefore, the transfer function of the phase lead controller is shown in (20).

$$G_c(s)=3\frac{s+2.37}{s+7.1} \tag{20}$$

Bode plot of the compensated system and the simulation results are shown in Figs. 6 (solid line) and 7, respectively. For a 0.2 p.u. load change ($\Delta P_L=0.2$ p.u.), with a communication delay of 0.5s, both the ACE signal and $\Delta\omega$ show increasing in the amplitude of the oscillation (dash line), which means the system is unstable. By using the proposed compensator (shown as solid line in Fig. 7), $\Delta\omega$ can quickly settle to the desired value 0 with negligible oscillations. The ACE signal also has a good performance with an overshoot less than 0.01 p.u. and a short settling period as well.

4.2. Multi-area LFC

For a multi-area LFC scheme, as described in Section 3.3, the equivalent design can be achieved if (18) is satisfied. Two simulations are carried out and discussed: a five-area system based on data from a 68-bus system [28], and a ten-area LFC system extended from the aforementioned five-area system. The five-area system simulation study illustrates the effectiveness of the proposed method in multi-area LFC schemes. Simulation results on the ten-area system show that the proposed method can be applied to large systems in practice even if the coupling among each area becomes stronger as the size of the system increases, i.e., the number of control areas gets larger.

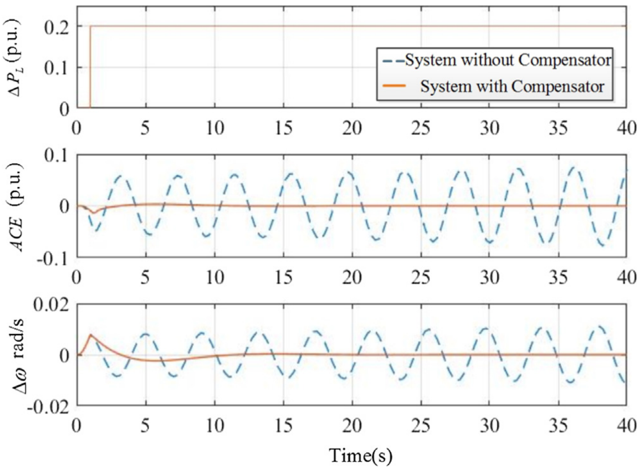

Fig. 7. One-area system response of 0.5s delay following a 0.2 p.u. load change using proposed compensator (Solid) and without compensator (Dash).

4.2.1. Five-area LFC using 68-bus system data

Simulation is carried out based on the IEEE 68-bus system with a total 16 generators in 5 different areas. In this 5-area, 68-bus system, the New York power system (NYPS) has four generators and the New England test system (NETS) has nine generators while the other three areas are represented by their corresponding equivalent single-generator models. The following procedures can be taken to obtain the parameters of the equivalent single-generator models for the NYPS and the NETS [29]:

$$D_{i,o} = \sum_{k=1}^{n_i} D_{ik,o};\quad M_{i,o} = \sum_{k=1}^{n_i} M_{ik,o};\quad \beta_{i,o} = \sum_{k=1}^{n_i} \left(D_{ik,o} + \frac{1}{R_{ik,o}}\right)$$

Notations of D, M, R, and β are the same as those used in Section 2.1.

To convert the parameters to a new base $S_{base} = 1000$ MVA, the following equations can be used:

$$D_i = \frac{S_{base,o}}{S_{base}} D_{i,o};\quad M_i = \frac{S_{base,o}}{S_{base}} M_{i,o};\quad R_i = \frac{S_{base}}{S_{base,o}} R_{i,o}$$

Therefore, equivalent single-generator models of NYPS and NETS can be obtained and parameters of the five-area system are given in Table 2.

Based on parameters given in Table 2, values of $||\Delta_5||_\infty$ and $\frac{1}{||N_5^{-1}||_\infty}$ are calculated to be 0.173 and 0.917, respectively, which satisfy (19). Simulation results of the five-area system are shown in Fig. 8. Due to space limit, only Areas 1, 3, and 5 are shown. Fig. 8 indicates the scenario that the communication delays exist in all five areas. Increasing oscillations in ACE, $\Delta\omega$ and P_{tie} in all three areas imply communication delays do negatively impact the system performance and stability. The system responses without compensators show that the system loses its stability in all five areas. With the compensators that are designed for each area separately, as shown by the solid line, the impacts of delays are mitigated, and the whole system remains stable. All the responses shown in Fig. 8 can be quickly settled down in a short period of time with negligible oscillations.

4.2.2. Ten-area LFC with time-varying delay

Since delays can happen in a random way [30], time-varying random delays which changes within the range $[\tau_{max}/3, \tau_{max}]$ are used in this simulation study ($\tau_{max} = 12s$). The delay compensator can be designed for the worst-case scenario so that, theoretically, the impact of any delay smaller than τ_{max} can be mitigated [24]. In the ten-area LFC system, different time-varying random delay was added to each area. As previously discussed, when the condition of (18) is met, the design process is much simplified for the ten-area system and the delay compensator for each area can be quickly designed based on the procedure give in Section 4.

By checking $||\Delta_{10}||_\infty$ and $1/||N_{10}^{-1}||_\infty$ of this ten-area system, we can find that the condition in (18) also holds. Hence, we can design the delay compensator for each control area separately. Only three areas' responses are shown in Fig. 9 with the τ_{max} in these three areas being 10s, 8s, 11s, respectively. The solid line indicates the proposed method can still mitigate the impact of time-varying random delay with a fast settling time and small oscillations. Nevertheless, it should be noted that the system can become more closely coupled when more control areas are connected together. More discussions on this are given in the following section.

5. Discussion

5.1. Comparison with LMI method

As discussed in Section 3, a controller is guaranteed to be found by using the proposed approach since it provides the necessary and sufficient stability condition. In contrast, the widely-used LMI approaches proposed in [4,14] only provide a sufficient condition, which does not tell how to design a controller and cannot guarantee its existence. The following example shows the advantages of our approach compared with the LMI method used in the LFC control in [14]. It was claimed in the paper that the LMI is feasible when $K_P = 0$, $K_I = 0.4$ for τ between [3.1s, 3.4s] by implementing Theorem 1 in [14]. In other words, if the delay keeps increasing and goes beyond its upper bound of 3.4s, e.g., $\tau = 4.0s$, the LMI approach will become infeasible. In that case, no controller can be found or designed by using the LMI approach. However, by applying the proposed method in this paper, a compensator can be identified for the same system when $\tau = 4.0s$. Simulation results shown in Fig. 10 clearly indicate the scenario mentioned above.

5.2. Couplings in multi-area LFC scheme

Couplings among different areas can significantly impact performance of the load frequency control for the entire system. Coupling are typically determined by the system topology (e.g., whether there is a tie-line and the corresponding line parameters), system operating condition (e.g., the synchronizing power coefficients), and system control parameters (e.g., the integral gains K_I). In this paper, (15) or (18) can be used to determine if the proposed method can still be used to design delay compensator for each area separately. An example is given in Fig. 11a to illustrate how the coupling index I_n ($||N_n^{-1}\Delta_n||_\infty$) changes based on the number of areas increased. The example value of $||N_n^{-1}\Delta_n||_\infty$ has been calculated based on the following two assumptions:

(1) For simplicity of analysis, each area is assumed to have the same set of parameters and the couplings between any two areas are the same.
(2) In an n-area system, each area is connected with the other n-1 areas. In other words, every two areas are connected, which is the scenario with the strongest possible coupling among different areas. Considering the H-infinity norm of a matrix is determined by its maximum sum of the elements in each row, interconnections between every two areas guarantee scenarios simulated representing

Table 2
Parameters of five-area LFC scheme.

Para.	M_i	D_i	β_i	R_i	K_{Ii}	T_{gi}	T_{chi}	ΔP_{Li}
$Area_1$	30	0.8	20.8	0.05	0.3	0.2	0.5	0.20
$Area_2$	30	1.0	19	0.0556	0.3	0.3	0.6	0.10
$Area_3$	65	3	84	0.0125	0.1	0.2	0.5	0.25
$Area_4$	45	1.2	17.2	0.0625	0.3	0.4	0.6	0.15
$Area_5$	56.52	0.72	58	0.02	0.2	0.2	0.5	0.20

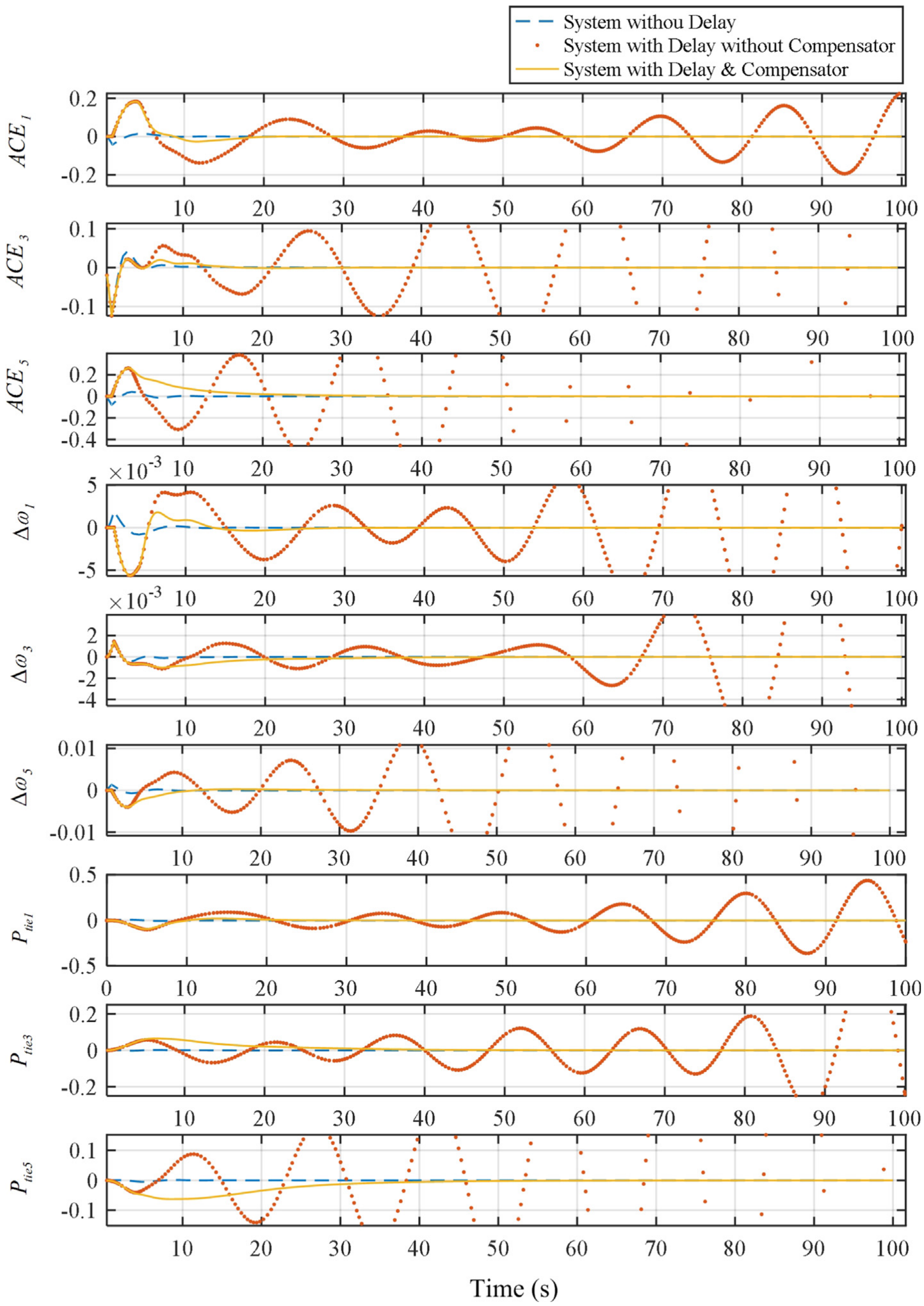

Fig. 8. Proposed method in a 5-area system. The communication delay in each area is 4 s, 5 s, 4 s, 6 s, 3 s, respectively.

the extreme condition of the index I_n ($\|\boldsymbol{N_n^{-1}}\Delta_n\|_\infty$) in a multi-area scheme.

Fig. 11 shows that for the example multi-area systems, a delay compensator can be designed for each area independently without considering the coupling among areas since (18) is satisfied. Fig. 11 shows that as the number of areas increases, the value of $\|\boldsymbol{\Delta_n}\|_\infty$ is getting closer to $1/\|\boldsymbol{N_n^{-1}}\|_\infty$. Moreover, it is reasonable to assume that not all the sub areas are connected in a practical LFC scheme and this may also help further decrease the value of $\|\boldsymbol{N_n^{-1}}\Delta_n\|_\infty$. The proposed method cannot deal with the situation when the condition (index) of (18) is not satisfied. If such index exceeds the upper limit, the coupling among different areas is then deemed too strong. Under this situation, it is suggested that other approaches should be used to achieve the control target. Nevertheless, the case studies in this paper show that the indices for the strongly coupled systems (i.e., there is a tie line between any two areas) are below the threshold value. In other words, even for those highly coupled systems, the proposed method can still be used. Our future work will be focused on developing delay compensators for LFC of renewable power plants and virtual power plants via the aggregation of heterogeneous sources.

6. Conclusion

In this paper, an alternative approach is proposed for designing delay compensators for LFC schemes of large power systems with communication delays. Different from LMI approaches, the proposed method gives a sufficient and necessary condition (i.e., $\tau < \varphi_\omega/\omega_c$) for designing delay compensator for a one-area LFC scheme. The study has also been extended to multi-area LFC schemes that covers a wide area. The criterion has been established based on the small gain theorem for designing controllers independently for individual areas/subsystems in

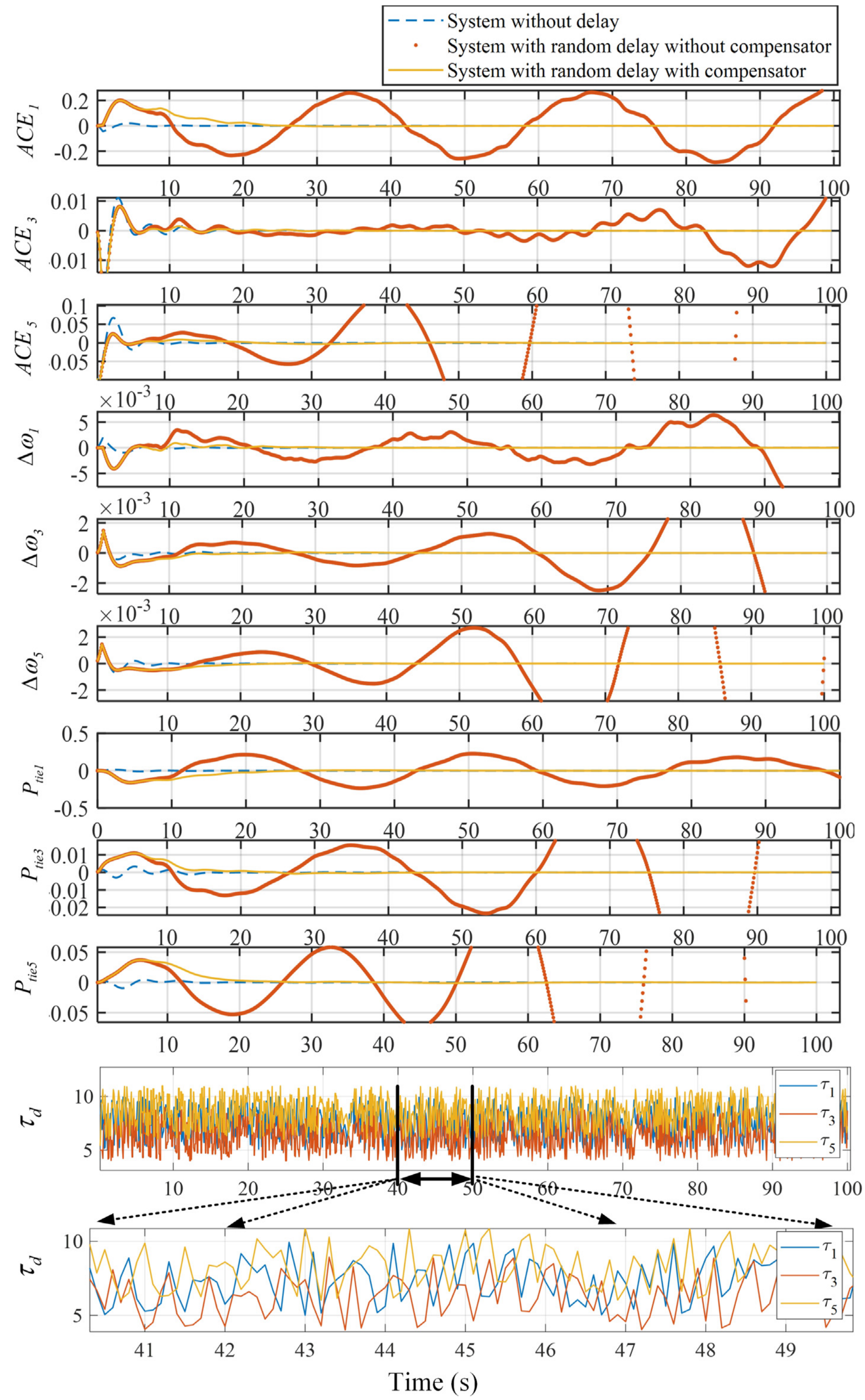

Fig. 9. 10 area system LFC with random delay (Only three areas are shown. The time-varying random delays in these three areas are shown at the bottom of this figure).

a multi-area system while the overall system stability is guaranteed. If the criterion is met, the delay compensator design procedure can be much simplified since each area can just deal with its own time delay. The effectiveness of the proposed method has been verified by simulation studies under different scenarios for both one-area and multi-area LFC systems subject to random delays. Discussions have been given on the comparison of this method and typical LMI approaches. The couplings among different control areas have been further discussed for implementation of the proposed approach to bulk power systems.

Declaration of Competing Interest

The authors declare that they have no known competing financial interests or personal relationships that could have appeared to influence the work reported in this paper.

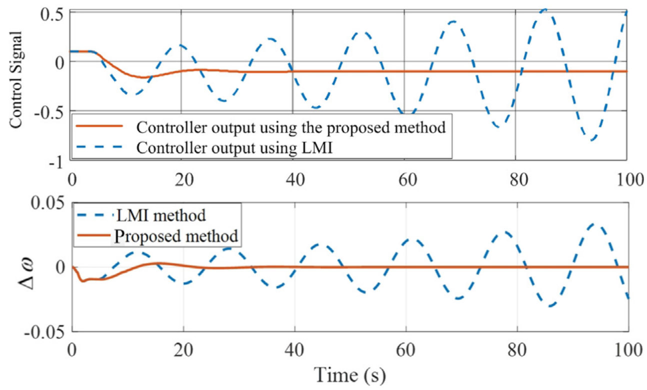

Fig. 10. The comparison between the proposed method and the LMI method when delay $\tau = 4.0$ s.

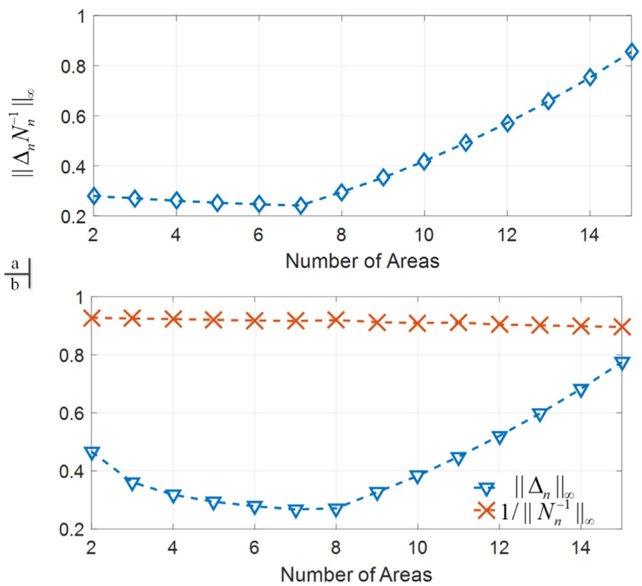

Fig. 11. Calculated $\|N_n^{-1}\Delta_n\|_\infty$ value and comparison, up to 15-area LFC.

References

[1] Saadat H. Power system analysis. 2nd Edition The McGraw-Hill Companies; 2002.

[2] Wen G, Hu G, Hu J, Shi X, Chen G. Frequency regulation of source-grid-load systems: a compound control strategy. IEEE Trans Industr Inf 2016;12(1):69–78. https://doi.org/10.1109/TII.2015.2496309.

[3] Ibraheem P, Kumar DP. Kothari, Recent philosophies of automatic generation control strategies in power systems. IEEE Trans Power Syst 2005;20(1):346–57. https://doi.org/10.1109/TPWRS.2004.840438.

[4] Tomsovic K, Bakken DE, Venkatasubramanian V, Bose A. Designing the next generation of real-time control, communication, and computations for large power systems. Proc IEEE 2005;93(5):965–79. https://doi.org/10.1109/JPROC.2005.847249.

[5] Olivares DE, Mehrizi-Sani A, Etemadi AH, Cañizares CA, Iravani R, Kazerani M, Hajimiragha AH, Gomis-Bellmunt O, Saeedifard M, Palma-Behnke R, Jiménez-Estévez GA, Hatziargyriou ND. Trends in microgrid control. IEEE Trans Smart Grid 2014;5(4):1905–19. https://doi.org/10.1109/TSG.2013.2295514.

[6] Yao W, Jiang L, Wen J, Wu Q, Cheng S. Wide-area damping controller for power system interarea oscillations: a networked predictive control approach. IEEE Trans Control Syst Technol 2015;23(1):27–36. https://doi.org/10.1109/TCST.2014.2311852.

[7] Lu K, Zhou W, Zeng G, Zheng Y. Constrained population extremal optimization-based robust load frequency control of multi-area interconnected power system. Int J Electric Power Energy Syst 2019;105:249–71. https://doi.org/10.1016/j.ijepes.2018.08.043.

[8] Sumithra M, Vinitha MJC, Mary DTJ. Controller design for single area load frequency control with time delays using genetic algorithm. Int J Appl Eng Res 2018;13:11909–16.

[9] Jin L, Zhang C, He Y, Jiang L, Wu M. Delay-dependent stability analysis of multi-area load frequency control with enhanced accuracy and computation efficiency. IEEE Trans Power Syst 2019;34(5):3687–96. https://doi.org/10.1109/TPWRS.2019.2902373.

[10] Wen S, Yu X, Zeng Z, Wang J. Event-triggering load frequency control for multiarea power systems with communication delays. IEEE Trans Industr Electron 2016;63(2):1308–17. https://doi.org/10.1109/TIE.2015.2399394.

[11] Ahumada C, Cérdenas R, Séez D, Guerrero JM. Secondary control strategies for frequency restoration in islanded microgrids with consideration of communication delays. IEEE Trans Smart Grid 2016;7(3):1430–41. https://doi.org/10.1109/TSG.2015.2461190.

[12] Yu X, Tomsovic K. Application of linear matrix inequalities for load frequency control with communication delays. IEEE Trans Power Syst 2004;19(3):1508–15. https://doi.org/10.1109/TPWRS.2004.831670.

[13] Yang F, He J, Wang D. New stability criteria of delayed load frequency control systems via infinite-series-based inequality. IEEE Trans Industr Inf 2018;14(1):231–40. https://doi.org/10.1109/TII.2017.2751510.

[14] Jiang L, Yao W, Wu QH, Wen JY, Cheng SJ. Delay-dependent stability for load frequency control with constant and time-varying delays. IEEE Trans Power Syst 2012;27(2):932–41. https://doi.org/10.1109/TPWRS.2011.2172821.

[15] Zhang CK, Jiang L, Wu QH, He Y, Wu M. Delay-dependent robust load frequency control for time delay power systems. IEEE Trans Power Syst 2013;28(3):2192–201. https://doi.org/10.1109/TPWRS.2012.2228281.

[16] Xiong L, Li H, Wang J. Lmi based robust load frequency control for time delayed power system via delay margin estimation. Int J Electrical Power Energy Syst 2018;100:91–103. https://doi.org/10.1016/j.ijepes.2018.02.027.

[17] Singh VP, Kishor N, Samuel P. Improved load frequency control of power system using lmi based pid approach. J Franklin Inst 2017;354(15):6805–30. https://doi.org/10.1016/j.jfranklin.2017.08.031.

[18] Ojaghi P, Rahmani M. Lmi-based robust predictive load frequency control for power systems with communication delays. IEEE Trans Power Syst 2017;32(5):4091–100. https://doi.org/10.1109/TPWRS.2017.2654453.

[19] Dey R, Ghosh S, Ray G, Rakshit A. H_∞ load frequency control of interconnected power systems with communication delays. Int J Electrical Power Energy Syst 2012;42(1):672–84.

[20] Ahmadi A, Aldeen M. An lmi approach to the design of robust delay-dependent overlapping load frequency control of uncertain power systems. Int J Electrical Power Energy Syst 2016;81:48–63. https://doi.org/10.1016/j.ijepes.2016.02.001.

[21] Boyd S, El Ghaoui L, Feron E, Balakrishnan V. Linear matrix inequalities in system and control theory vol. 15. Siam; 1994.

[22] Zhou K, Doyle JC, Glover K, et al. Robust and optimal control vol. 40. New Jersey: Prentice hall; 1996.

[23] Terkovics N, Neild SA, Lowenberg M, Szalai R, Krauskopf B. Substructurability: the effect of interface location on a real-time dynamic substructuring test, Proc Roy Soc Lond A: Math Phys Eng Sci 472 (2192). doi:10.1098/rspa.2016.0433.

[24] Ogata K, Yang Y. Modern control engineering. NJ: Prentice-Hall Englewood Cliffs; 1970.

[25] Zames G. On the input-output stability of time-varying nonlinear feedback systems part one: conditions derived using concepts of loop gain, conicity, and positivity. IEEE Trans Autom Control 1966;11(2):228–38. https://doi.org/10.1109/TAC.1966.1098316.

[26] Fu C, Wang C, Wang L, Zhao B. Control of pv systems for distribution network voltage regulation with communication delays. Electric Power Syst Res 2020;179:106071.

[27] Fu C. Analysis and mitigation of the impacts of delays in control of power systems with renewable energy sources Ph.D. thesis Wayne State University; 2019.

[28] Singh AK, Pal BC. IEEE PES task force on benchmark systems for stability controls report on the 68-bus, 16-machine, 5-area system; 2013. http://eioc.pnnl.gov/benchmark/ieeess/.

[29] Zhang Y, Dong L, Gao Z. Load frequency control for multiple-area power systems. In: American Control Conference, 2009. ACC'09., IEEE; 2009. p. 2773–8.

[30] Zhang X-M, Han Q-L, Yu X. Survey on recent advances in networked control systems. IEEE Trans Industr Inf 2016;12(5):1740–52.